






Article

Selection of suitable bentonite and the influence of various acids on the preparation of a special clay for the removal of trace olefins from aromatics

Hadi Rouhani^{1†}, Fatola Farhadi¹ , Mahsa Akbari Kenari^{1†}, Effat Eskandari²  and Seeram Ramakrishna^{3*} 

¹Chemical and Petroleum Engineering Department, Sharif University of Technology, Tehran, Iran; ²Department of Geology, Faculty of Science, Ferdowsi University of Mashhad, Mashhad, Iran and ³Center for Nanotechnology and Sustainability, Department of Mechanical Engineering, National University of Singapore, Singapore 117581, Singapore

Abstract

Acid-activated clays are inexpensive materials that are used extensively in the removal of unsaturated compounds on an industrial scale. The performance of bentonitic clays in removing these compounds relies heavily on the types of raw clays and acids used in the activation process. In this work, we report on the removal of olefins from aromatic streams by bentonitic clays activated *via* two different routes. After preliminary tests of four different natural clays, the best clay was selected in terms of it having high swelling index, cation-exchange capacity, specific surface area and suspension stability values. Activation was achieved with hydrochloric acid (HCl) and sulfuric acid (H₂SO₄), and olefin removal was evaluated after holistic clay characterization by means of X-ray diffraction, X-ray fluorescence, Brunauer–Emmett–Teller (BET) specific surface area analysis, ζ-potential analysis, Fourier-transform infrared (FTIR) spectroscopy after treatment with pyridine, scanning electron microscopy and transmission electron microscopy. The increased basal spacing, replacement of H⁺ with interlayer cations and retained structural stability of the clay after acid treatment contributed to the improvement of olefin removal for HCl-activated clay. The HCl-activated clay was more efficient in terms of olefin removal than its H₂SO₄-activated counterpart, removing up to 90% of olefin components after 40 h. Based on pyridine-FTIR spectra and quantitative measurement of the acidic properties of the samples, HCl treatment increased the total number acid sites (Brønsted and Lewis) by approximately ninefold compared to the pristine natural clay and by approximately fourfold compared to the H₂SO₄-activated clay.

Keywords: acid-activated bentonite, acid treatment, bentonite, interlayer cations, olefin removal

(Received 5 May 2021; revised 19 October 2021; Accepted Manuscript online: 1 December 2021; Associate Editor: Miroslav Pospíšil)

Colloidal inorganic particles with a size of <2 μm are generally classified as clays regardless of their composition and crystal structure (Rautureau *et al.*, 2017; Stawinski, 2017; Guo *et al.*, 2020). Bentonite is a clay with multiple applications in the oil, gas, petrochemical, food, pharmaceutical, building and agriculture industries (Mannu *et al.*, 2018; Abuchenari *et al.*, 2020; Javed *et al.*, 2020; Rouhani & Farhadi, 2020; Qureshi *et al.*, 2021; Shakiba *et al.*, 2021). The main mineral constituent of bentonite is montmorillonite, a member of the smectite group (Chen *et al.*, 2019). Montmorillonite is a layer silicate consisting of an octahedral sheet with aluminium as a principal cation placed between two tetrahedral sheets with silicon as the main cation (Fig. 1) (Schoonheydt *et al.*, 2018; Fayoyiwa, 2020). Cations such as Fe³⁺ and Mg²⁺ may replace Al³⁺ in the octahedral sheet and Al³⁺ may replace Si⁴⁺ in the tetrahedral sheets (Prandel *et al.*, 2017; Vaculíková *et al.*, 2019). Because of these substitutions, montmorillonite bears a negative layer charge. Cations such as Na, Ca, Mg and K enter the interlayer space to neutralize

the negative charge. These cations adsorb water between the layers and are readily exchanged, contributing to the cation-exchange capacity (CEC) of the clay (Pérez-Cabrera *et al.*, 2019; Leporatti *et al.*, 2020).

Montmorillonite is an efficient adsorbent of heavy metals and is easily activated by inorganic acids such as sulfuric acid (H₂SO₄) and hydrochloric acid (HCl) (Balci, 2016; Abdellaoui *et al.*, 2019; Hao *et al.*, 2019; Qin *et al.*, 2020). During activation, H⁺ ions substitute for exchangeable cations, and Al³⁺ and other octahedral and tetrahedral cations of montmorillonite are released, whereas SiO₄ units remain intact (Al-Essa, 2018; Sims, 2019; Elmorsi *et al.*, 2021).

Two major types of bentonites have been reported in the literature. In the sodium-rich bentonites, montmorillonite contains exchangeable Na and adsorbs water readily. Thus, it is stable in dilute suspensions, forming gels (Uddin, 2018; Hayakawa *et al.*, 2019; Kumar & Lingfa, 2020). The calcium-rich bentonites (where calcium is the major cation of montmorillonite) absorb less water and thus swell less than the Na-rich bentonites (Mahmoud *et al.*, 2018; Uddin, 2018; Yang *et al.*, 2018). X-ray diffraction (XRD) and the swelling index are used for bentonite characterization (Andrini *et al.*, 2017; Monteiro *et al.*, 2018; Özgüven *et al.*, 2020).

Physical and chemical modifications of clays that improve their properties are known as ‘activation processes’. One type of

[†]These authors contributed equally to this work

*E-mail: mpestr@nus.edu.sg

Cite this article: Rouhani H, Farhadi F, Akbari Kenari M, Eskandari E, Ramakrishna S (2021). Selection of suitable bentonite and the influence of various acids on the preparation of a special clay for the removal of trace olefins from aromatics. *Clay Minerals* 56, 185–196. <https://doi.org/10.1180/clm.2021.32>

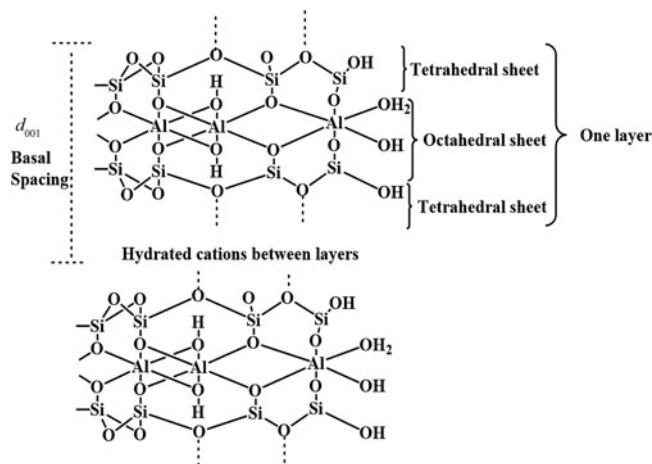


Fig. 1. Crystal structure of montmorillonite.

activation process is acid activation by mineral acids such as H_2SO_4 and HCl (Samudrala *et al.*, 2018; Dutta, 2019). Upon acid activation, protons penetrate the clay layers and attack their structural OH groups. The subsequent dehydroxylation occurs through the sequential release of central atoms from octahedral cell units as well as the removal of Al^{3+} from tetrahedral sheets. Consequently, the tetrahedral sheets are gradually transformed into three-dimensional frameworks. The resultant solid product comprises partially dissolved layers and amorphous silica, depending on the intensity of activation, whereas the ambient acid solution contains ions that depend on the chemical composition of the clay material and the acid employed. Acid-treated clay minerals always produce various reaction products with enhanced catalytic properties (Carrado & Komadel, 2009; Komadel & Madejová, 2013; Yu *et al.*, 2017; Huang *et al.*, 2019; Balbay *et al.*, 2021). A schematic representation of the acid activation process of montmorillonite is shown in Fig. 2.

Petroleum processing produces aromatic streams containing benzene, toluene and xylene during reforming and cracking processes. The production of these compounds is accompanied by the production of undesirable olefins that can be harmful to downstream units and poison their catalysts (Liu *et al.*, 2017; Wang *et al.*, 2021).

Two processes are typically used for the removal of olefins from aromatic streams: (1) clay treating and (2) catalytic hydrotreating (Liu *et al.*, 2017; Guo *et al.*, 2020). In catalytic hydrotreating, olefins are saturated during the hydrogenation reactions on selective hydrogenation catalysts. In the clay-treating process, the acidic ability of the clay leads to the separation of olefins from aromatics according to the Friedel–Crafts alkylation reaction

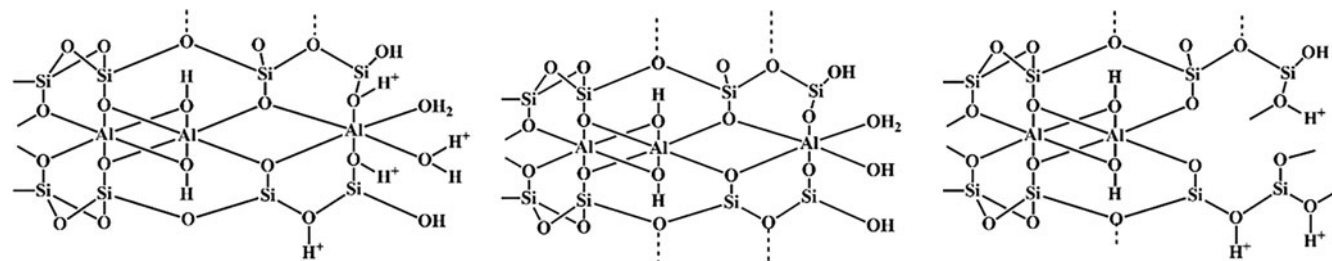


Fig. 2. Representation of the acidic process on montmorillonite.

Table 1. Aromatic hydrocarbon component analysis.

Component	wt. %
Non-aromatics	7.65
Benzene	29.52
Toluene	60.10
Ethylbenzene	0.11
p-Xylene	0.18
m-Xylene	0.34
o-Xylene	0.13
C9 and C9+	1.95

(Xin *et al.*, 2018; Choudhary *et al.*, 2020). Clay treating is commonly used for separating olefins from aromatic streams because catalytic hydrotreating is associated with considerable olefin losses only at greater temperatures and pressure conditions, thus raising operating costs (Emam, 2018; Wu *et al.*, 2018; Wang *et al.*, 2021).

In the present study, the most suitable bentonite was selected among four different materials after the evaluation of the swelling index, CEC, specific surface area and suspension stability. Previous studies focused on the preparation of activated clays by adding metal halides or other compounds through processes that were time-consuming, not environmentally friendly and not cost-efficient (Li *et al.*, 2011; Luan *et al.*, 2011; Choudhury, 2020). The selected bentonite was activated using two different acids (HCl and H_2SO_4) and was used to eliminate olefins from a hydrocarbon mixture. The activated clays and the natural clay were characterized using XRD, X-ray fluorescence (XRF), Brunauer–Emmett–Teller (BET) specific surface area analysis, ζ -potential, Fourier-transform infrared (FTIR) spectroscopy after treatment with pyridine (pyridine-FTIR), scanning electron microscopy (SEM) and transmission electron microscopy (TEM). Olefin removal was also examined in pilot tests. The efficiency of the desired sample (HCl -activated bentonite) was demonstrated according to these analyses. Pyridine-FTIR was used for the first time to elucidate the mechanism of trace olefin removal from an aromatic stream by acid-activated clay. Moreover, this work proposes a method of selection of the most suitable bentonite for the removal of olefins from aromatics based on a series of analyses. Ultimately, the HCl -activated bentonite yielded a conversion rate of olefins of $\sim 95\%$ after 48 h, which is significantly greater than has been previously reported.

Experimental

Materials

Natural bentonite samples were obtained from various mines of Iran, namely Nasimab 1 (N-1), Nasimab 2 (N-2), Abgarm



Fig. 3. (a) The ball mill and (b) the vibration sieve shaker for preparing the raw bentonite samples.

Table 2. Swelling index, CEC and BET specific surface area values of the bentonite samples.

Property	Sample			
	A	N-1	N-2	K
Swelling index (mg 2 g ⁻¹ clay)	10.0	9.0	15.5	23.0
CEC (meq 100 g ⁻¹ clay)	55	60	64	80
BET specific surface area (m ² g ⁻¹)	26.10	27.50	29.90	37.65

(A; Semnan province) and Kheyrahad (K; Kerman province). All chemicals (sodium chloride, ethylene amine copper, HCl and H₂SO₄) were of analytical grade (Merck, Germany). Aromatic hydrocarbons were obtained from Bou Ali Sina (Avicenna) petrochemical company for pilot tests. The composition analysis was accomplished by gas chromatography (GC; Varian CP-3800) according to ASTM D-5134 with Cpsil CB column ($L = 50$ m, $d = 0.5$ μ m) (Table 1). The conditions for the GC analysis were oven temperature 75–280°C, inlet injection temperature 250°C and flame ionization detector temperature 250°C.

Selection of the suitable bentonite

The samples were ground with a ball mill (Cross Beater Mill SK 100, Retsch Co., Germany) and sieved so that ~80% passed through a 200 mesh (74 μ m) sieve (Fig. 3). The samples were then dried at 110°C for 12 h.

The swelling index, CEC, BET specific surface area and ζ -potential analyses were conducted to determine the most suitable bentonite for the acid treatment. The first test conducted on fine bentonite samples was the swelling index. Because calcium bentonite has a low specific surface area, this test was necessary to select the most suitable sample (Yu *et al.*, 2021). The swelling index test was conducted according to ASTM D-5890 and 2 g of each sample were added to 100 mL of deionized water and the volume of the gel formed was measured after 24 h (Table 2) (Rouhani *et al.*, 2016). Bentonite sample K is Na-rich and the remaining bentonites are Ca-rich. To further support the results of the swelling test, the ζ -potential was determined to measure the suspension stability of the raw clays. Bentonite sample K is more stable than the remaining samples with a ζ -potential of ~-48 mV, compared to the ζ -potential value of ~0 mV for the remaining bentonites (Fig. 4). Hence, bentonite sample K

suspensions would be more stable during the acid-treatment process than the other bentonite suspensions (El-Geundi *et al.*, 1995; Dikmen *et al.*, 2012). Moreover, the CEC and BET specific surface area analyses demonstrated the suitability of bentonite sample K as a promising sample for activation (Table 2). Therefore, bentonite sample K was selected for further study because of its high CEC, high BET specific surface area, promising swelling index value and stability.

Acid-treatment process

Acid treatment of natural clays improves their performance and increases their specific surface area, thereby improving their ultimate catalytic performance. In this work, HCl and H₂SO₄ were used for the acid-treatment process due to their significant impact on improving the properties of bentonite sample K (Komadel, 2003; Carrado & Komadel, 2009; Komadel & Madejová, 2013).

Acid activation was carried out using 4 M HCl and 4 M H₂SO₄. Greater acid concentrations may lead to the destruction of the smectite structure, while lower concentrations may not create a specific surface area that is suitable for activation (Christidis *et al.*, 1997; Finevich *et al.*, 2007). A total of 5 g of the bentonite was stirred magnetically with 100 mL of each acid for 8 h at 85°C in a round-bottomed flask under total reflux conditions to prevent acid evaporation (Fig. 5a). The temperature was kept constant using a heater and thermometer that were checked regularly. The slurry was cooled by air, centrifuged and washed with distilled water until the pH and conductivity of the washing water were stable and sufficiently close to the respective values for distilled water (Fig. 5b) (Christidis *et al.*, 1997).

Filtered samples were collected and dried at 120°C for 6 h (Fig. 5c). The activated samples were labelled as 'HClA' for HCl-activated clay and 'HSA' for H₂SO₄-activated clay, while natural bentonite was labelled as 'NC' for natural clay.

Determination of CEC

The CEC values of the samples were determined using the copper ethylenediamine method (Bergaya & Vayer, 1997). Copper ethylenediamine complex solution was obtained by mixing 1 M NaCl and ethylene amine copper, and the product solution was diluted to 0.01 M. Then 25 mL of solution was stirred with 0.5 g of natural clay for ~30 min, and the obtained suspension was filtered. The concentration of copper in the filtrate was measured using atomic

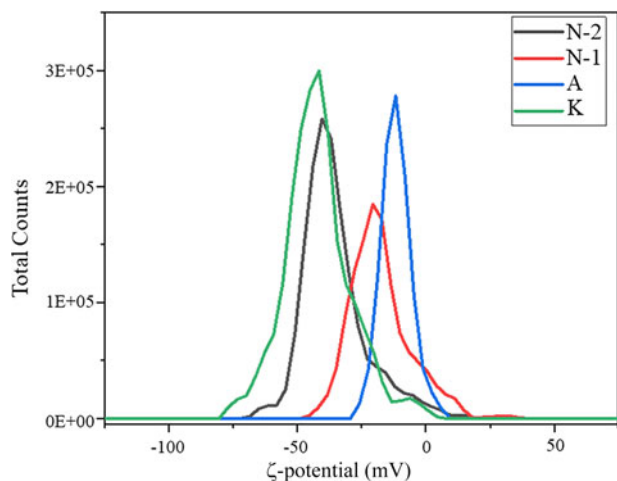


Fig. 4. ζ -potential values of the raw bentonites.

absorption spectroscopy. The CEC values were determined according to the absorption of copper in the sample (Bergaya & Vayer, 1997; Rihayat *et al.*, 2018). Acid treatment reduced the CEC values (Table 3). HCl reduced the CEC values more than H_2SO_4 .

Catalyst test in a pilot plant

Dried samples were crushed with a pestle and mortar after cooling and screened to 20–40 mesh. The screened samples were placed in an oven at 120°C for 100 min. Finally, samples were prepared for loading into the reactor (Fig. 6a).

Catalytic tests of the treated and natural clays were conducted in a pilot plant (Fig. 6c). A total of 7.7 g of each sample was loaded in a stainless-steel reactor equipped with a flow controller and a heating system. Samples were placed between two quartz sand layers and ceramic balls (40–60 mesh) in the reactor (Fig. 6d). The reaction was carried out at 185°C , a reaction pressure of 16 bar and a weight hourly space velocity (WHSV) of 6.56 h^{-1} (Rouhani & Farhadi, 2020).

The olefin contents of the feed and product streams were measured using the bromine index (BI) in accordance with ASTM D 2710-92. The BI is defined as the number of milligrams of bromine consumed by 100 g of a hydrocarbon sample (Pu *et al.*, 2012).

The conversion of olefins was calculated according to the following equation:

$$X = \left[\frac{\text{Br}_i - \text{Br}_o}{\text{Br}_i} \right] \times 100 \quad (1)$$

where Br_i and Br_o are the olefin contents of the feed and products, respectively ($o = 1, 2, 3, \dots$).

The feed of the clay-treating unit contains a typical BI of ~ 300 – 700 , which must be reduced to < 20 for industrial processes (Fig. 7) (Reddy *et al.*, 2020). In order to measure the olefin contents of the feed and product streams, the device demonstrated in Fig. 6b was used.

Results and discussion

XRF analysis of the bentonite samples

The acid activation process replaces interlayer ions (Ca^{2+} , Na^+ , K^+ , Mg^{2+}) with H^+ and increases the catalytic activity of the sample (Rouhani *et al.*, 2016). Table 4 lists the XRF analyses (using an Advant ARL (Thermo Electron SA Company, Switzerland) sequential X-ray fluorescence spectrometer) of two acid-activated samples compared to NC. The decrease in Na_2O content is shown in Table 3, indicating interlayer cations of montmorillonite (mainly sodium) were exchanged with H^+ . The decreases in MgO and Al_2O_3 after the acid treatment indicate that parts of the octahedral sheets were dissolved during activation. Many acid sites (Lewis and Brønsted) are created in montmorillonite through acid activation (Yang *et al.*, 2020; Dill *et al.*, 2021). The CaO , K_2O and Fe_2O_3 contents of the natural samples also decreased, indicating the impact of acid treatment on accessory minerals in the bentonite. The increase in SiO_2 after acid treatment indicates that tetrahedral Si^{4+} cations are not significantly leached by the acid treatment.

XRD analysis of the bentonite samples

The XRD traces (Equinox 3000, Inel Co., France) of the raw and acid-activated clays are shown in Fig. 8a. In addition to montmorillonite as the major mineral, minor cristobalite, hematite, calcite, illite and quartz are present in the bentonite (Fig. 8b) (Rouhani *et al.*, 2016). The XRD traces of the various samples are comparable, suggesting that the acid activation did not significantly disrupt the structure of



Fig. 5. (a) Preparation setup of the activated clays. (b) Device for measuring the conductivity of distilled water. (c) Acid-activated clay after drying.

Table 3. The CEC values of the raw and acid-activated bentonite samples.

Property	Sample		
	NC	HClA	HSA
CEC (meq 100 g ⁻¹ clay)	80	52	64

the montmorillonite. The d_{001} basal spacings of the NC and activated clays with H₂SO₄ and HCl are 10.70, 12.16, and 12.64 Å, respectively (Boulaouche *et al.*, 2019). Hence, during activation, the basal spacing increased by ~2 Å, and activation with HCl increased the basal spacing to a greater extent than activation with H₂SO₄ (Rouhani *et al.*, 2016).

The 001 peak intensity at ~9°2θ after acid activation decreased compared to that of NC, suggesting that acid activation modified the structure of the montmorillonite. The intensities of the non-basal (prismatic) reflections at ~20°2θ (110) and at 62°2θ (060) also decreased slightly. Hence, the crystal order of the samples decreased slightly during acid activation.

BET analysis of the bentonite samples

The N₂ adsorption–desorption isotherms of the samples are shown in Fig. 9. All isotherms are type IV according to the International Union of Pure and Applied Chemistry (IUPAC) classification (Amari *et al.*, 2018). Table 5 lists the BET specific surface area (BEL Japan, Inc.), total pore volume and pore diameter values of three clay samples. The BET specific surface area

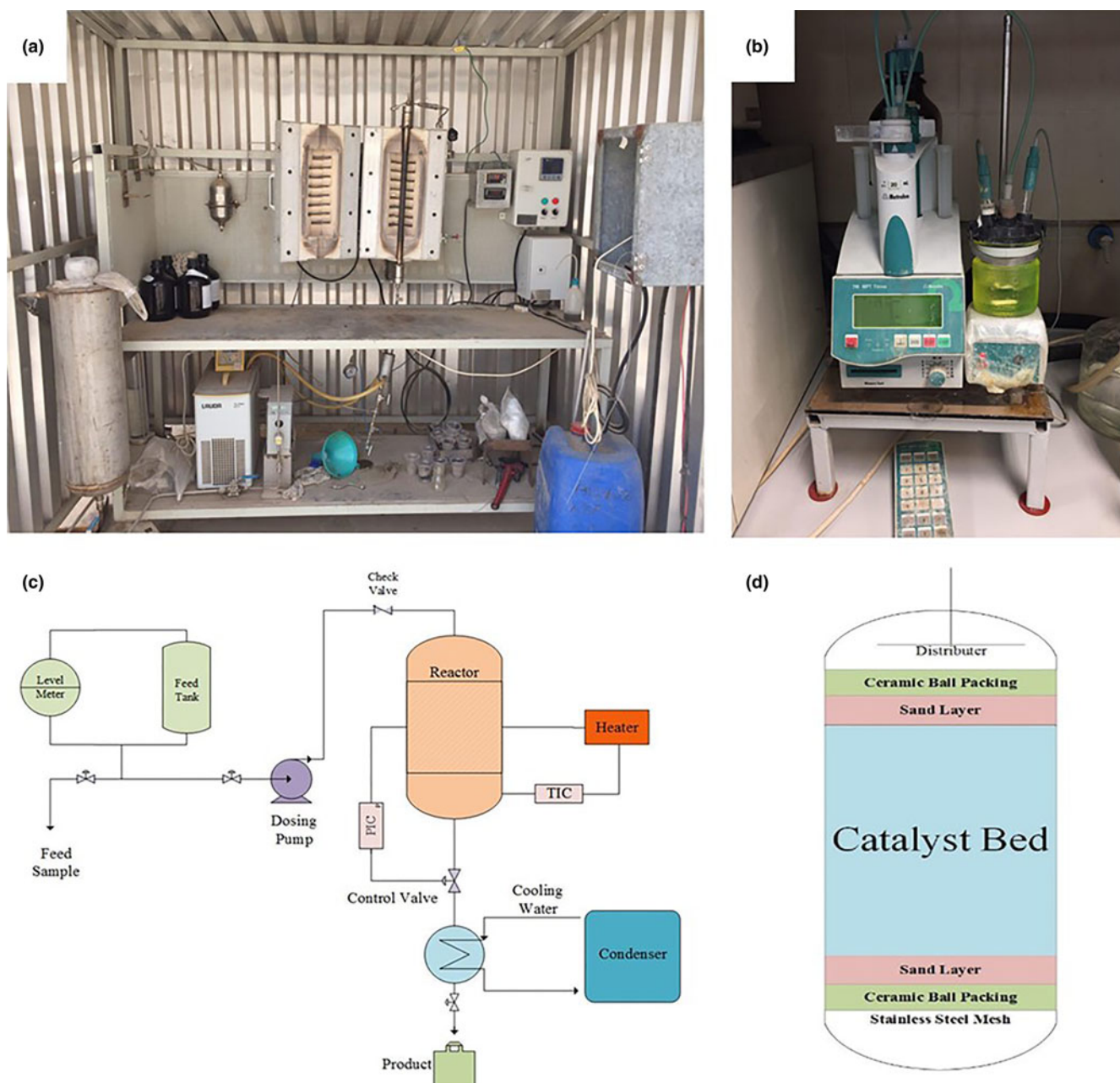


Fig. 6. (a) Photograph of the pilot plant for olefin removal by clays for testing the prepared samples. (b) Titration device for measuring the BI of the feed and product samples. (c) Overall schematic of the pilot plant. (d) Internal structure of the reactor.

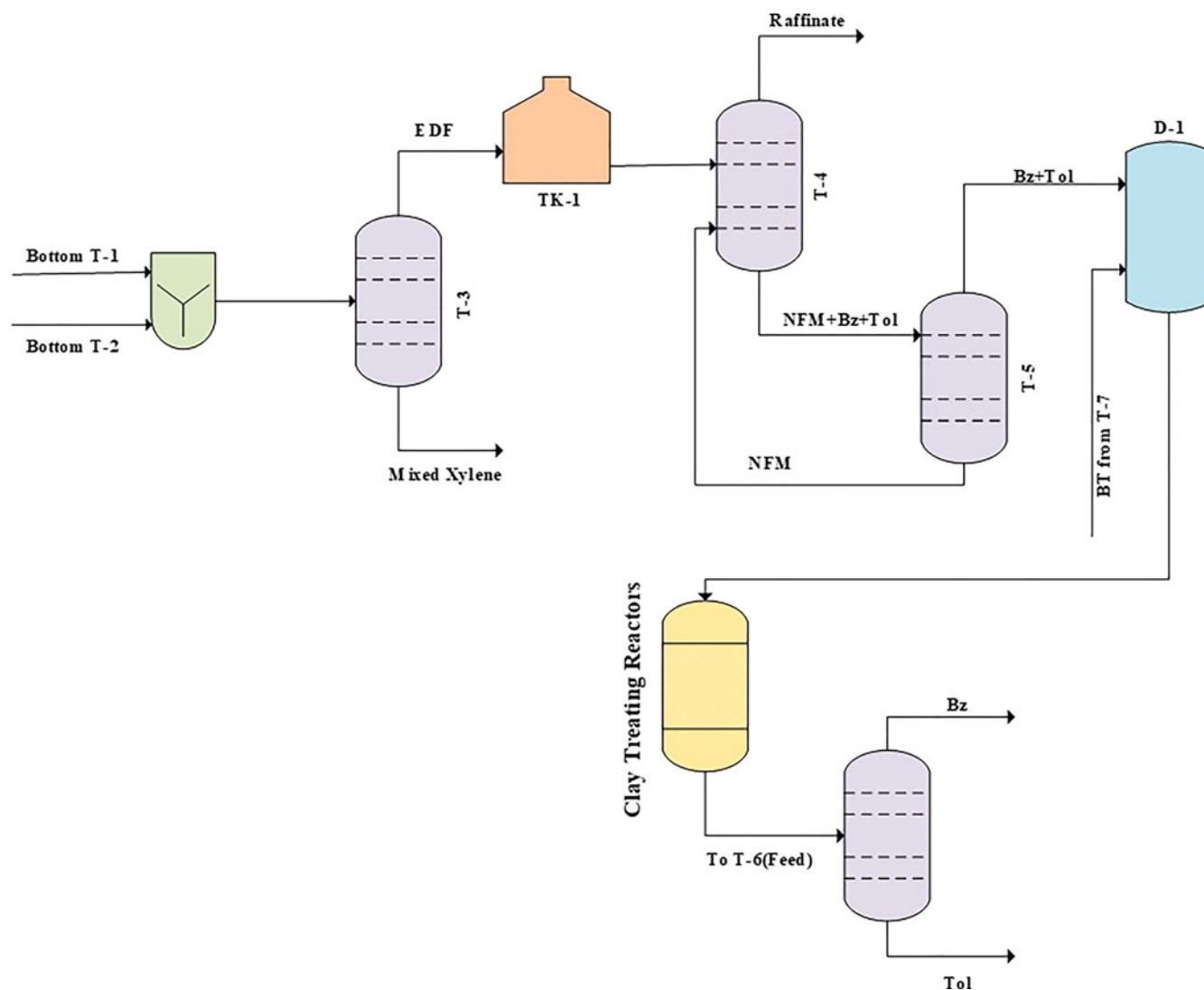


Fig. 7. Flow diagram of the clay-treatment unit in a petrochemical plant. BT = benzene and toluene mixture; Bz = benzene; EDF = extractive distillation feed; NFM = normal formylmorpholine; Tol = toluene.

increased during acid activation with both acids. The total pore volume of the samples also increased during acid activation, but the pore diameter of the activated samples decreased. Generally, a reduction in mean pore diameter may cause an increase in total pore volume, and these results are in accordance with this theory (Obayomi & Auta, 2019). Acid treatment with HCl increased the BET specific surface area and total pore volume to a greater extent than did acid treatment with H_2SO_4 .

Pyridine-FTIR spectra of the bentonite samples

The concentration of acidic sites was determined *via* quantitative FTIR spectroscopy using the KBr method with pyridine as the probe molecule. The KBr discs in the cell were heated at 653 K under vacuum for 2 h and cooled to 353 K for pyridine adsorption. The sample was then subjected to thermal desorption at 723 K to remove pyridine, followed by FTIR measurement (Tensor 27, Bruker Co., MA, USA) (Li *et al.*, 2011; Luan *et al.*, 2011). The FTIR spectra for the pyridine adsorption of samples are shown in Fig. 10, and the calculated concentrations of acid sites are given in Table 6.

Table 4. XRF analysis of the bentonite samples.

Composition	Sample		
	NC (wt.%)	HClA (wt.%)	HSA (wt.%)
SiO_2	70.400	76.500	76.400
Al_2O_3	11.100	9.500	9.100
MgO	2.400	1.560	1.470
Fe_2O_3	3.560	3.200	2.860
CaO	1.460	0.200	0.450
Na_2O	1.790	0.200	0.058
K_2O	0.340	0.140	0.180
TiO_2	0.310	0.260	0.280
P_2O_5	0.024	0.007	0.008
SO_3	0.054	0.004	0.150
MnO	0.050	0.008	0.006
LOI	8.512	8.421	9.038

LOI = loss on ignition.

The FTIR spectra displayed several characteristic bands in the 1400–1600 cm^{-1} range, which are attributed to the interaction of pyridine with Lewis and Brønsted acid sites on the sample surface.

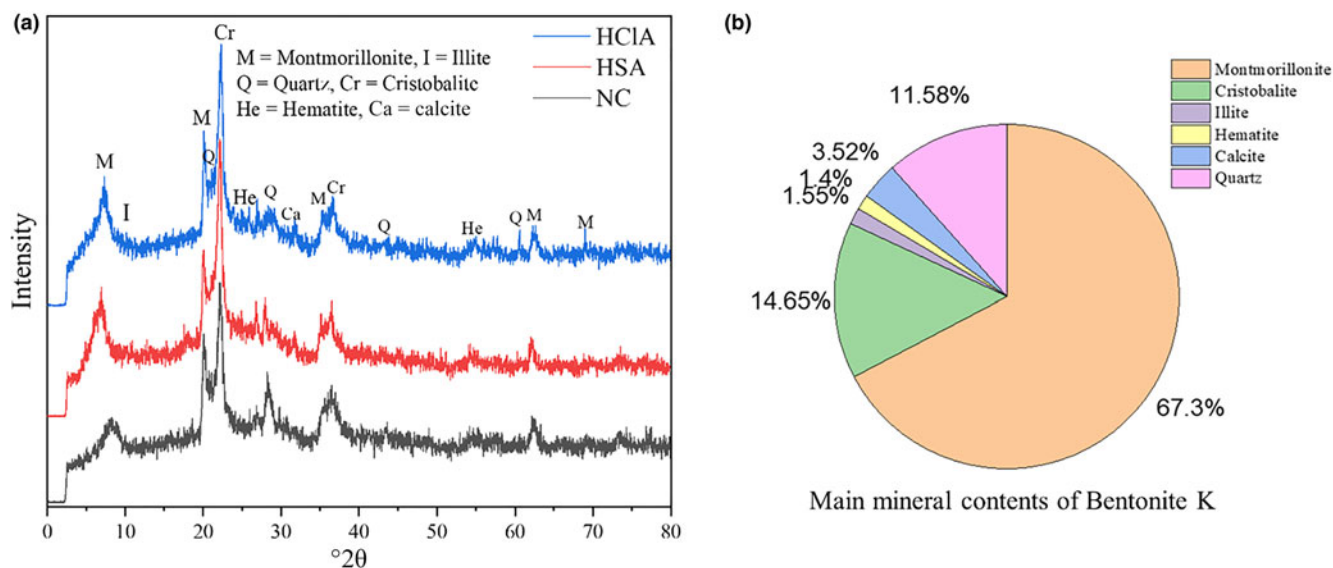


Fig. 8. (a) XRD traces of the NC and activated clays. (b) Quantitative mineralogical composition of the NC (bentonite K).

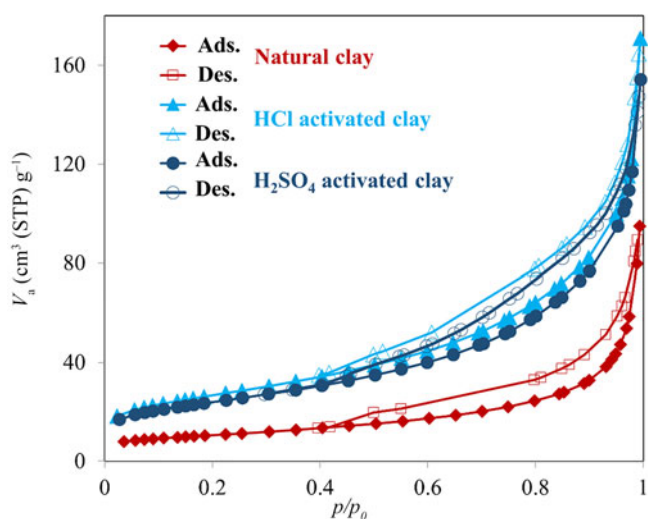


Fig. 9. N_2 adsorption-desorption isotherms of the bentonite samples. For each sample, the lower lines correspond to adsorption (Ads.) and the upper lines correspond to desorption (Des.). STP = standard temperature and pressure.

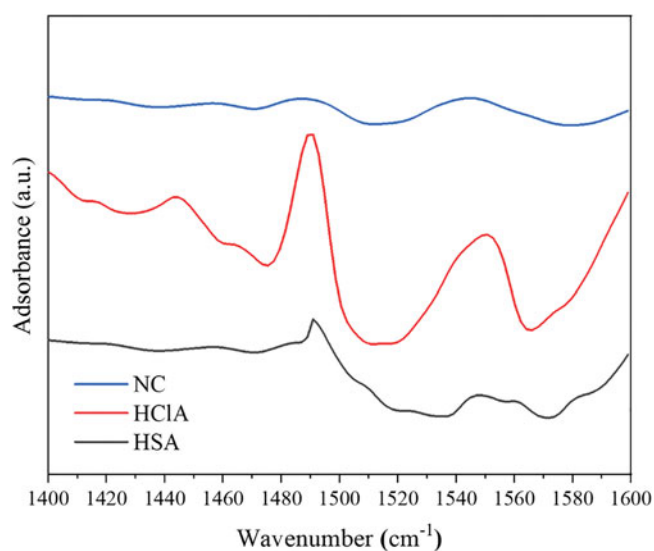


Fig. 10. FTIR spectra of pyridine adsorbed on the various bentonite samples at 723 K.

Table 5. Textural properties of the bentonite samples.

Sample	Surface area ($m^2 g^{-1}$)	Pore volume ($cm^3 g^{-1}$)	Pore diameter (nm)
NC	37.65	0.1308	13.394
HSA	161.8	0.2994	10.222
HClA	195.3	0.3438	10.163

The band at $\sim 1450 cm^{-1}$ is due to pyridine adsorbed on the Lewis acid sites, while the band at $1490 cm^{-1}$ is due to contributions of both the Lewis and Brønsted acid sites. Finally, the band at $\sim 1540 cm^{-1}$ is due to pyridine adsorbed on Brønsted acid sites (Li *et al.*, 2011; Luan *et al.*, 2011). The concentrations of Brønsted and Lewis acid sites were calculated from the integrated absorbance intensities of these bands (Fig. 10).

Table 6. Acidic properties of the bentonite samples.

Sample	Amount of acid sites ($\times 10^{-4} mol g^{-1}$)		
	Total acid sites	Total Lewis acid sites	Total Brønsted acid sites
NC	0.08206	0.02238	0.05222
HClA	0.71989	0.15293	0.56696
HSA	0.19396	0.02984	0.16412

The FTIR bands of the HCl-activated clay are more intense, indicating stronger acidic properties of this sample compared to its counterparts (Fig. 10). The acid treatment had a strong influence on the acidic properties of the samples (Table 6) and increased the number of Lewis acid sites. In addition, activation with HCl created more Lewis acid sites than did activation with

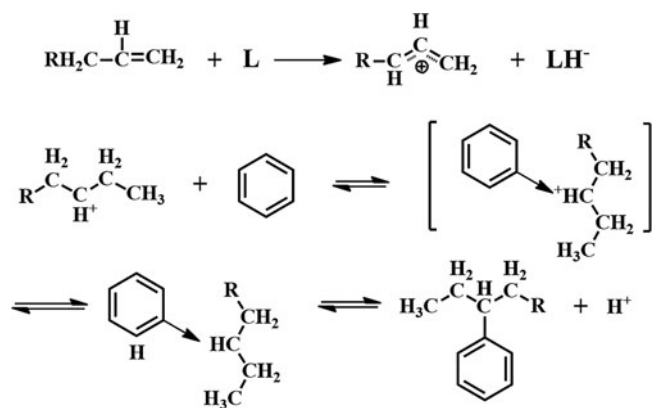


Fig. 11. Mechanism of reaction between olefins and aromatics.

H_2SO_4 . The alkylation of aromatics with olefins over a catalyst generally obeys the carbonium ion mechanism (Fig. 11). Hence, the Lewis acid sites acted as the catalysts of the alkylation reaction in this mechanism and the olefin molecule was protonated by the Lewis acid sites. The olefin molecule was turned into a carbonium ion through electrophilic attack on the aromatic π -electrons, a

mono- or poly-alkylbenzenium ion. The desorption process and the loss of the proton yielded the alkylated aromatic and restored the Lewis acid sites (Pu *et al.*, 2012).

SEM and TEM images of the bentonite samples

SEM images (AIS 2100 SEM, SERON Technologies, Korea) of the samples (NC, H_2SO_4 -activated and HCl-activated) are shown in Fig. 12. The NC consists of thick irregular platelets partly forming chunks or flakes. The acid-treated samples consist of smaller ragged or serrated particles, highlighting the effect of acid erosion. Leaching of interlayer cations during acid treatment and their replacement by H^+ ions potentially affected the edges of the platelets, which became wider and more open (Selvitepe *et al.*, 2019). However, in the TEM images, the lamellar structure of the NC was retained after acid treatment (Fig. 13). Hence, the thick platelets and multilayers of the clay were converted to thin and single-layer crystallites.

Effect of acid treatment on catalytic activity

The olefin separation performances of the NC and acid-treated samples are compared in Fig. 14, whereby the conversion (%) of olefins was determined according to Equation 1. Acid treatment had a significant impact on the catalytic activity of the

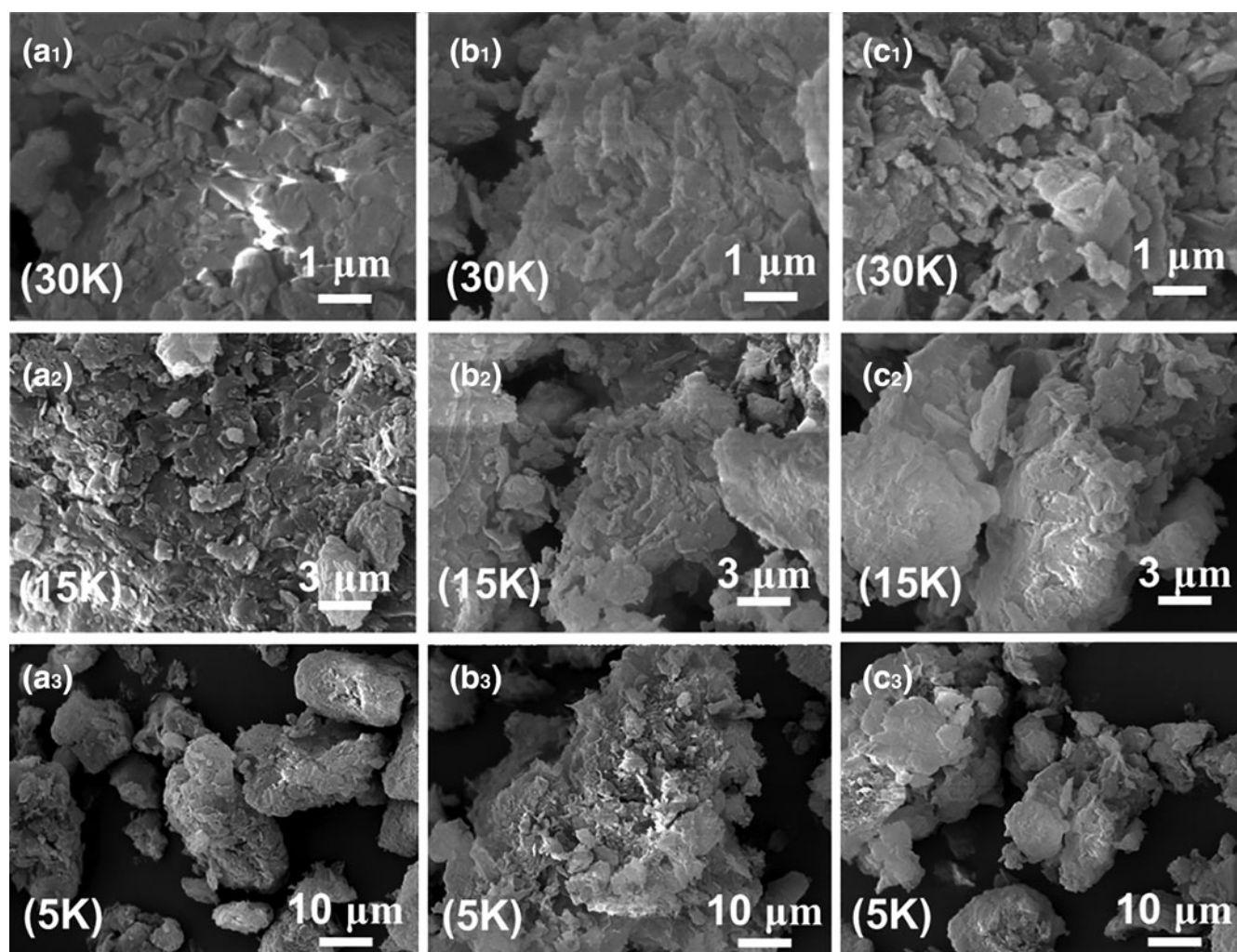


Fig. 12. SEM images of (a₁-a₃) NC (30,000× magnification), (b₁-b₃) H_2SO_4 -activated clay (15,000× magnification) and (c₁-c₃) HCl-activated clay (5000× magnification).

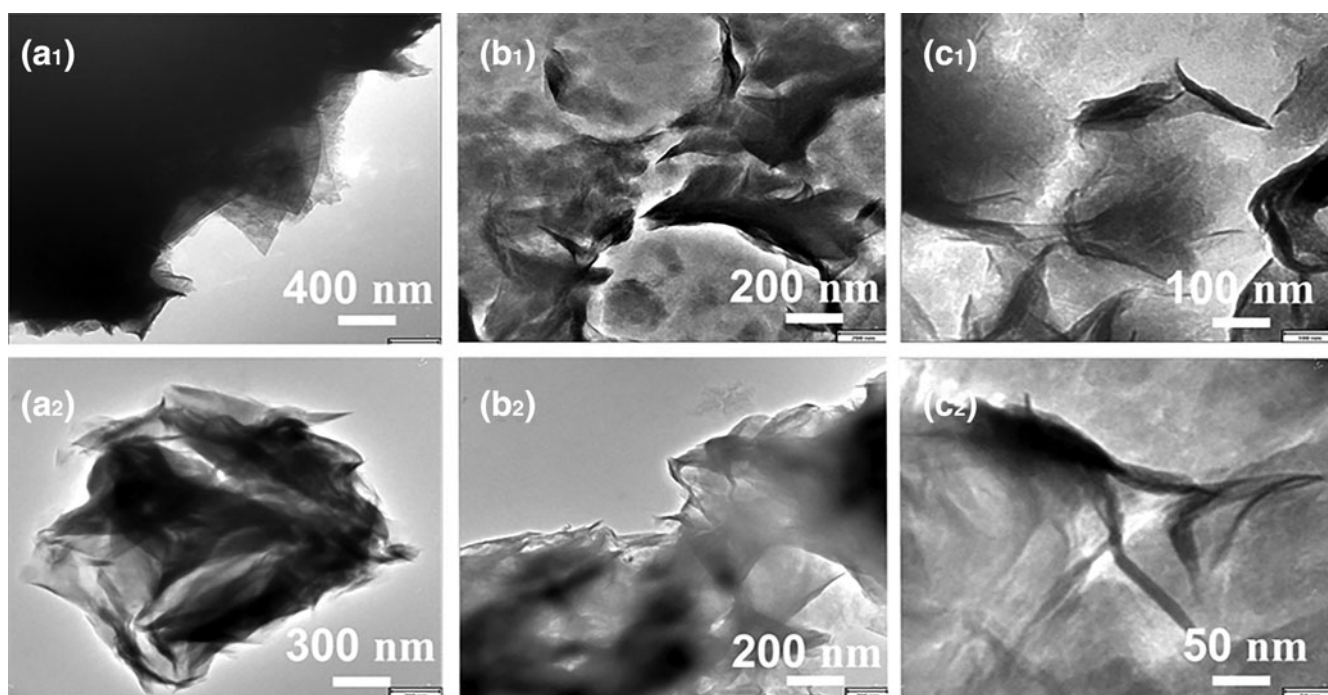


Fig. 13. TEM images of (a₁ & a₂) NC, (b₁ & b₂) H₂SO₄-activated clay and (c₁ & c₂) HCl-activated clay.

bentonite, such that the number of Lewis acid sites of the clay increased, leading to a several-fold decrease in the operating time compared to that of NC. The NC did not reduce the BI value to <20, while the acid-activated samples were effective in this respect. In addition, HClA demonstrated a better conversion rate of olefins than did HSA. Hence, acid treatment with HCl created a greater number of acid sites than did H₂SO₄, which agrees strongly with the characterization results.

The conversion rate of olefins decreased with time, probably due to deactivation of acid sites, especially Lewis acid sites. Previous work has shown that N-formylmorpholine, morpholine and water, which exist in the feed stream of the reactor, act as poisons for the clay and deactivate the Lewis acid sites (Rouhani & Farhadi, 2020). Therefore, the conversion of olefins is reduced with time. The original bentonite had a small number of acid sites (Table 6); therefore, it converted olefins only by 73% and was deactivated after ~10 h (Fig. 14). A comparison between the clays prepared in this study and materials from similar studies is given in Table 7. The HClA from this study obtained an

olefin conversion rate of ~93% after 48 h under a WHSV of 6.56 h⁻¹, which is much greater than that reported in the literature with expensive materials and extensive preparation methods (Li *et al.*, 2011; Luan *et al.*, 2011; Pu *et al.*, 2012). Therefore, HClA may be used at a commercial scale due to the simplicity of its activation and its facile preparation. As HClA can maintain olefin conversion for a longer period of time than HSA, deactivation of clay would be delayed and, consequently, the annual amount of disposed deactivated clay would be reduced. Hence, this material is environmentally friendly and cost-effective for industrial use.

Summary and conclusions

The removal of olefins from a hydrocarbon mixture was successfully accomplished due to the catalytic and adsorption ability of an acid-activated bentonite. The performance of activated clays (HClA and HAS) was compared with a natural clay by means of several analytical methods, namely BI conversion (%), XRD,

Table 7. Comprehensive comparison of the olefin removal rates of the prepared special clays with results from the literature.

Sample	Olefin conversion (%)	Reaction duration (h)	WHSV (h ⁻¹)	Reference
Clay + 10% metal halides	80%	3	30	Li <i>et al.</i> (2011)
Clay + 7% metal halides	84%	3	30	Luan <i>et al.</i> (2011)
Zeolite (MCM-22) + 7% La ₂ O ₃	78%	3	30	Pu <i>et al.</i> (2012)
Ionic liquid ([BuPy]Br-AlCl ₃)	92.5%	10	–	Sun <i>et al.</i> (2011)
Acid-activated Al-pillared bentonite	98%	4.5	–	Faghihian & Mohammadi (2014)
Sulfated zirconia	91%	8	30	Yao <i>et al.</i> (2015)
Mesoporous materials + AlCl ₃	84%	10	30	Chen <i>et al.</i> (2009)
CoCl ₂ -modified acid-activated palygorskite	92%	7	30	Guo <i>et al.</i> (2020)
Zeolite-based catalyst	95%	10	2.1	Reddy <i>et al.</i> (2020)
Acid-modified Y zeolite (ReUSY)	90%	30	10	Yu <i>et al.</i> (2020)
HClA	93%	48	6.56	This work

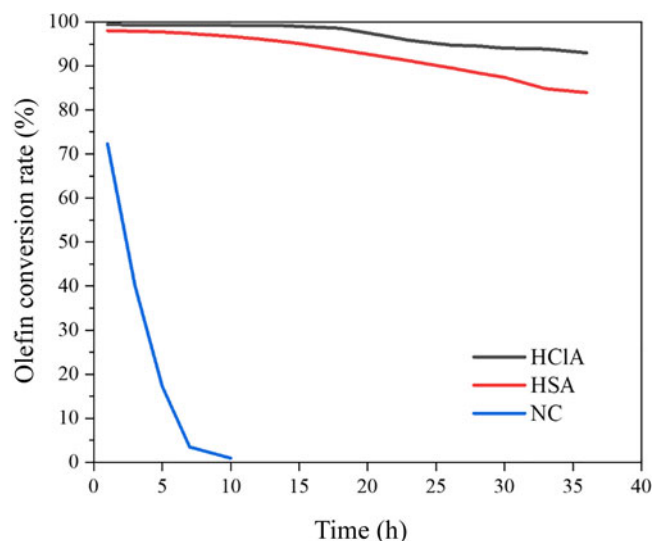


Fig. 14. Effect of the acid-treatment procedure on the conversion of olefins.

XRF, BET specific surface area, pyridine-FTIR, SEM and TEM. The acid treatment produced acid sites in the montmorillonite interlayer via replacement of Na, Ca and K by H^+ . The HClA sample was more effective for the removal of olefins from aromatics than its counterparts. This sample showed more extensive replacement of interlayer cations by H^+ and a more pronounced increase in the montmorillonite 001 basal spacing than did the HSA sample. Acid treatment with HCl increased the BET specific surface area and total pore volume to a greater extent than did acid treatment with H_2SO_4 . The HCl-activated clay had sharper absorbance intensities in the FTIR spectra after sorption of pyridine due to its greater number of acid sites compared to the other samples. The edges of the flakes in the NC were eroded by acid treatment, producing wider pores and thinner sheets. Overall, these characterization results are complementary with those of the catalytic performance test. Treatment of clays with HCl is more efficient than treatment with H_2SO_4 for removing olefinic components from a mixed stream of hydrocarbons. This study demonstrated the effect of activation with various acids on bentonites and introduced a cost-effective, environmentally friendly and simple method in comparison with previous studies.

Supplementary material. To view supplementary material for this article, please visit <https://doi.org/10.1180/clm.2021.32>.

References

- Abdellaoui Y., Olguín M.T., Abatal M., Ali B., Méndez S.E.D. & Santiago A.A. (2019) Comparison of the divalent heavy metals (Pb, Cu and Cd) adsorption behavior by montmorillonite-KSF and their calcium-and sodium-forms. *Superlattices Microstructures*, **127**, 165–175.
- Abuchenari A., Hardani K., Abazari S., Naghdi F., Keleshteri M.A., Jamavari A. & Chahardehi A.M. (2020) Clay-reinforced nanocomposites for the slow release of chemical fertilizers and water retention. *Journal of Composites Compounds*, **2**, 85–91.
- Al-Essa, K. (2018) Activation of Jordanian bentonite by hydrochloric acid and its potential for olive mill wastewater enhanced treatment. *Journal of Chemistry*, **2018**, 8385692.
- Amari A., Gannouni H., Khan M.I., Almesfer M.K., Elkhaleefa A.M. & Gannouni A. (2018) Effect of structure and chemical activation on the adsorption properties of green clay minerals for the removal of cationic dye. *Applied Sciences*, **8**, 2302.

- Andrini L., Toja R.M., Gauna M.R., Conconi M.S., Requejo F.G. & Rendtorff N. (2017) Extended and local structural characterization of a natural and 800°C fired Na-montmorillonite-Patagonian bentonite by XRD and Al/Si XANES. *Applied Clay Science*, **137**, 233–240.
- Balbay A., Selvitepe N. & Saka C. (2021) Fe doped-CoB catalysts with phosphoric acid-activated montmorillonite as support for efficient hydrogen production via $NaBH_4$ hydrolysis. *International Journal of Hydrogen Energy*, **46**, 425–438.
- Balci S. (2016) Structural property improvements of bentonite with sulfuric acid activation. *Journal of the Turkish Chemical Society Section B: Chemical Engineering*, **1**, 201–212.
- Bergaya F. & Vayer M. (1997) CEC of clays: measurement by adsorption of a copper ethylenediamine complex. *Applied Clay Science*, **12**, 275–280.
- Boulaouche T., Kherroub D.E., Khimeche K. & Belbachir M. (2019) Green strategy for the synthesis of polyurethane by a heterogeneous catalyst based on activated clay. *Research on Chemical Intermediates*, **45**, 3585–3600.
- Carrado K.A. & Komadel P. (2009) Acid activation of bentonites and polymer-clay nanocomposites. *Elements*, **5**, 111–116.
- Chen C., Wu W., Zeng X., Jiang Z. & Shi L. (2009) Study on several mesoporous materials catalysts applied to the removal of trace olefins from aromatics and commercial sidestream tests. *Industrial & Engineering Chemistry Research*, **48**, 10359–10363.
- Chen Y., Sun Z., Cui Y., Ye W. & Liu Q. (2019) Effect of cement solutions on the swelling pressure of compacted GMZ bentonite at different temperatures. *Construction Building Materials*, **229**, 116872.
- Choudhary T., Pham T.N. & Uppili S. (2020) *Highly Selective Olefin Removal with Un sulfided Hydrotreating Catalysts*. Patent and Trademark Office, Washington, DC. US Patent 10,562,829.
- Choudhury T. (2020) Clay hybrid materials. Pp. 17–32 in: *Clay Science and Technology* (G.M. Do Nascimento, editor). IntechOpen, London.
- Christidis G., Scott P. & Dunham A. (1997) Acid activation and bleaching capacity of bentonites from the islands of Milos and Chios, Aegean, Greece. *Applied Clay Science*, **12**, 329–347.
- Dikmen S., Yilmaz G., Yorukogullari E. & Korkmaz E. (2012) Zeta potential study of natural- and acid-activated sepiolites in electrolyte solutions. *Canadian Journal of Chemical Engineering*, **90**, 785–792.
- Dill L.P., Kochevka D.M., Lima L.L., Leitão A.A., Wypych F. & Cordeiro C.S. (2021) Brazilian mineral clays: classification, acid activation and application as catalysts for methyl esterification reactions. *Journal of the Brazilian Chemical Society*, **32**, 145–157.
- Dutta D.K. (2019) Recent advances in metal nanoparticles supported on montmorillonite as catalysts for organic synthesis. *Journal of Materials NanoScience*, **6**, 19–31.
- El-Geundi M., Ismail H. & Attyia K. (1995) Activated clay as an adsorbent for cationic dyestuffs. *Adsorption Science Technology*, **12**, 109–117.
- Elmorsi R.R., Mostafa G.A.H. & Abou-El-Sherbini K.S. (2021) Homoionic soda-activated bentonite for batch-mode removal of Pb(II) from polluted brackish water. *Journal of Environmental Chemical Engineering*, **9**, 104606.
- Emam E.A. (2018) Clay adsorption perspective on petroleum refining industry. *Industrial Engineering*, **2**, 19–25.
- Faghian H. & Mohammadi M.H. (2014) Acid activation effect on the catalytic performance of Al-pillared bentonite in alkylation of benzene with olefins. *Applied Clay Science*, **93**, 1–7.
- Fayoyiwa A.D. (2020) *The Effects of the Chemical Composition and Interlayer Cations on the Swelling Pressure of Smectite Clay Minerals: A Molecular Dynamics Study*. PhD dissertation. University of Eastern Finland, Kuopio, 49 pp.
- Finevich V., Allert N., Karpova T. & Duplyakin V. (2007) Composite nanomaterials on the basis of acid-activated montmorillonites. *Russian Journal of General Chemistry*, **77**, 2265–2271.
- Guo H., Zhang H., Li Q., Peng F., Xiong L., Wang C. et al. (2020) Removal of olefins from reforming aromatic hydrocarbons over metal-halide-modified acid-activated palygorskite. *Energy & Fuels*, **34**, 9463–9472.
- Hao J., Wei Z., Wei D., Mohamed T.A., Yu H., Xie X. et al. (2019) Roles of adding biochar and montmorillonite alone on reducing the bioavailability of heavy metals during chicken manure composting. *Bioresource Technology*, **294**, 122199.

- Hayakawa T., Oya M., Minase M., Fujita K.I., Teepakakorn A.P. & Ogawa M. (2019) Preparation of sodium-type bentonite with useful swelling property by a mechanochemical reaction from a weathered bentonite. *Applied Clay Science*, **175**, 124–129.
- Huang G.Q., Song Y.H., Liu C., Yang J.M., Lu J., Liu Z.T. & Liu Z.W. (2019) Acid activated montmorillonite for gas-phase catalytic dehydration of monoethanolamine. *Applied Clay Science*, **168**, 116–124.
- Javed U., Khushnood R.A., Memon S.A., Jalal F.E. & Zafar M.S. (2020) Sustainable incorporation of lime-bentonite clay composite for production of ecofriendly bricks. *Journal of Cleaner Production*, **263**, 121469.
- Komadel P. (2003) Chemically modified smectites. *Clay Minerals*, **38**, 127–138.
- Komadel P. & Madejová J. (2013) Acid activation of clay minerals. Pp. 385–409 in: *Developments in Clay Science* (F. Bergaya & G. Lagaly, editors). Elsevier, Amsterdam.
- Kumar A. & Lingfa P. (2020) Sodium bentonite and kaolin clays: comparative study on their FT-IR, XRF, and XRD. *Materials Today: Proceedings*, **22**, 737–742.
- Leporatti S., Cascione M., De Matteis V. & Rinaldi R. (2020) Design of nano-clays for drug delivery and bio-imaging: can toxicity be an issue? *Future Medicine*, **15**, 2429–2432.
- Li G., Luan J., Zeng X. & Shi L. (2011) Removal of trace olefins from aromatics over metal-halides-modified clay and its industrial test. *Industrial & Engineering Chemistry Research*, **50**, 6646–6649.
- Liu J., Liu N., Ren K., Shi L. & Meng X. (2017) Sulfated zirconia synthesized in a one step solvent-free method for removal of olefins from aromatics. *Industrial & Engineering Chemistry Research*, **56**, 7693–7699.
- Luan J., Li G. & Shi L. (2011) Study of modified clay and its industrial testing in aromatic refining. *Industrial & Engineering Chemistry Research*, **50**, 7150–7154.
- Mahmoud O., Nasr-El-Din H.A., Vryzas Z. & Kelessidis V.C. (2018) Effect of ferric oxide nanoparticles on the properties of filter cake formed by calcium bentonite-based drilling muds. *SPE Drilling Completion*, **33**, 363–376.
- Mannu A., Vlahopoulou G., Sireus V., Petretto G.L., Mulas G. & Garroni S. (2018) Bentonite as a refining agent in waste cooking oils recycling: flash point, density and color evaluation. *Natural Product Communications*, **13**, 613–616.
- Monteiro M.K.S., de Oliveira V.R.L., dos Santos F.K.G., de Barros Neto E.L., de Lima Leite R.H., Aroucha E.M.M. & de Oliveira Silva K.N. (2018) Influence of the ionic and nonionic surfactants mixture in the structure and properties of the modified bentonite clay. *Journal of Molecular Liquids*, **272**, 990–998.
- Obayomi K. & Auta M.J.H. (2019) Development of microporous activated Aloi clay for adsorption of lead (II) ions from aqueous solution. *Heliyon*, **5**, e02799.
- Özgüven F.E., Pekdemir A.D., Müşerref Ö. & Sarikaya Y. (2020) Characterization of a bentonite and its permanent aqueous suspension. *Journal of the Turkish Chemical Society Section A: Chemistry*, **7**, 11–18.
- Pérez-Cabrera L., Diaz-de-León J., Antúnez-García J., Galván D., Alonso-Núñez G. & Fuentes-Moyado S. (2019) Isomorphous substitution of Mg²⁺ by Al³⁺ on MgO: effects on basicity, textural properties and microstructure. *Revista Mexicana de Ingeniería Química*, **18**, 339–347.
- Prandel L.V., Dias N.M.P., da Costa Saab S., Brinatti A.M., Giarola N.F.B. & Pires L.F. (2017) Characterization of kaolinite in the hardsetting clay fraction using atomic force microscopy, X-ray diffraction, and the Rietveld method. *Journal of Soils Sediments*, **17**, 2144–2155.
- Pu X., Liu N., Jiang Z. & Shi L. (2012) Acidic and catalytic properties of modified clay for removing trace olefin from aromatics and its industrial test. *Industrial & Engineering Chemistry Research*, **51**, 13891–13896.
- Qin C., Yuan X., Xiong T., Tan Y.Z. & Wang H. (2020) Physicochemical properties, metal availability and bacterial community structure in heavy metal-polluted soil remediated by montmorillonite-based amendments. *Chemosphere*, **261**, 128010.
- Qureshi D., Behera K.P., Mohanty D., Mahapatra S.K., Verma S., Sukyai P. et al. (2021) Synthesis of novel poly (vinyl alcohol)/tamarind gum/bentonite-based composite films for drug delivery applications. *Colloids Surfaces A: Physicochemical Engineering Aspects*, **613**, 126043.
- Rautureau M., Gomes C.d.S.F., Liewig N. & Katouzian-Safadi M. (2017) Clay and clay mineral definition. Pp. 5–31 in: *Clays and Health: Properties and Therapeutic Uses*. Springer, Cham.
- Reddy J.K., Lad S., Mantri K., Das J., Raman G. & Jasra R.V. (2020) Zeolite-based catalysts for the removal of trace olefins from aromatic streams. *Applied Petrochemical Research*, **10**, 107–114.
- Rihayat T., Salim S., Arlina A., Fona Z., Jalal R., Alam P. et al. (2018) Determination of CEC value (cation exchange capacity) of bentonites from North Aceh and Bener Meriah, Aceh Province, Indonesia using three methods. P. 012054 in: *IOP Conference Series: Materials Science and Engineering* (Vol. 334, No. 1). IOP Publishing, Bristol.
- Rouhani H. & Farhadi F. (2020) Detecting and evaluating detrimental factors of clay's longevity, selecting, and optimizing an appropriate adsorbent for operating time elevation in the separation process of trace olefins from aromatics. *Industrial & Engineering Chemistry Research*, **59**, 2796–2804.
- Rouhani H., Sarrafi A. & Tahmoorei M. (2016) Synthesis of xanthene derivatives over acid activated clay in Kerman Province and kinetic modeling. *Chemical Engineering Communications*, **203**, 289–299.
- Samudrala S.P., Kandasamy S. & Bhattacharya S. (2018) Turning biodiesel waste glycerol into 1,3-propanediol: catalytic performance of sulphuric acid-activated montmorillonite supported platinum catalysts in glycerol hydrolysis. *Scientific Reports*, **8**, 7484.
- Schoonheydt R.A., Johnston C.T. & Bergaya F. (2018) Clay minerals and their surfaces. Pp. 1–21 in: *Developments in Clay Science* (F. Bergaya & G. Lagaly, editors). Elsevier, Amsterdam.
- Selvipte N., Balbay A. & Saka C. (2019) Optimisation of sepiolite clay with phosphoric acid treatment as support material for CoB catalyst and application to produce hydrogen from the NaBH₄ hydrolysis. *International Journal of Hydrogen Energy*, **44**, 16387–16399.
- Shakiba M., Kakoei A., Jafari I., Rezvani Ghomi E., Kalaei M., Zarei D. et al. (2021) Kinetic modeling and degradation study of liquid polysulfide resin-clay nanocomposite. *Molecules*, **26**, 635.
- Sims A.P. (2019) *Investigating Effect of Clay Composition on Safety Function Performance in a Geological Disposal Facility (GDF)*. PhD thesis. University of Manchester, 352 pp.
- Stawinski W.J. (2017) *Modified Clay Minerals as High-Effective Adsorbents for Wastewater Laden with Heavy Metals and Textile Dyestuffs*. University of Porto, 262 pp.
- Sun Y. & Shi L. (2011) Removal of trace olefins from aromatics at room temperature using pyridinium and imidazolium ionic liquids. *Industrial & Engineering Chemistry Research*, **50**, 9339–9343.
- Uddin F. (2018) Montmorillonite: an introduction to properties and utilization. Pp. 3–23 in: *Current Topics in the Utilization of Clay in Industrial and Medical Applications* (M. Zoveidavianpoor, editor). IntechOpen, London.
- Vaculíková L., Plevová E. & Ritz M. (2019) Characterization of montmorillonites by infrared and Raman spectroscopy for preparation of polymer-clay nanocomposites. *Journal of Nanoscience Nanotechnology*, **19**, 2775–2781.
- Wang L., Meng X., Wang S., Shi L., Hu X. & Liu N. (2021) Research and application of a non-noble metal catalyst in the removal of trace olefins from aromatics. *New Journal of Chemistry*, **45**, 3901–3908.
- Wu M., Han H., Ni L., Zhang S., Li S., Wang Y. et al. (2018) Mesoporous zirconium phosphonate hybrid bentonite as a novel efficient catalyst for the removal of trace olefins from aromatics. *Russian Journal of Applied Chemistry*, **91**, 758–763.
- Xin Q., Alvarez-Majmutov A., Dettman H.D. & Chen J. (2018) Hydrogenation of olefins in bitumen-derived naphtha over a commercial hydrotreating catalyst. *Energy & Fuels*, **32**, 6167–6175.
- Yang Y.L., Reddy K.R., Du Y.J. & Fan R.D. (2018) Sodium hexametaphosphate (SHMP)-amended calcium bentonite for slurry trench cutoff walls: workability and microstructure characteristics. *Canadian Geotechnical Journal*, **55**, 528–537.
- Yang F., Weng J., Ding J., Zhao Z., Qin L. & Xia F. (2020) Effective conversion of saccharides into hydroxymethylfurfural catalyzed by a natural clay, attapulgite. *Renewable Energy*, **151**, 829–836.

- Yao J., Liu N., Shi L. & Wang X. (2015) Sulfated zirconia as a novel and recyclable catalyst for removal of olefins from aromatics. *Catalysis Communications*, **66**, 126–129.
- Yu H., Zang J., Liu G., Hong M., Chen R. & Chen T. (2020) Acid-modified hierarchical porous rare-earth-containing Y zeolite as a highly active and stable catalyst for olefin removal. *ACS Omega*, **5**, 18028–18034.
- Yu C., Yang Y., Wu Z.X., Jiang J.F., Liao R. & Deng Y.F. (2021) Experimental study on the permeability and self-healing capacity of geosynthetic clay liners in heavy metal solutions. *Geotextiles Geomembranes*, **49**, 413–419.
- Yu W., Wang P., Zhou C., Zhao H., Tong D., Zhang H. *et al.* (2017) Acid-activated and WO_x-loaded montmorillonite catalysts and their catalytic behaviors in glycerol dehydration. *Chinese Journal of Catalysis*, **38**, 1087–1100.